Brain Topography (2019) 32:394–404
https://doi.org/10.1007/s10548-018-0678-z

ORIGINAL PAPER

Altered Dynamic Functional Network Connectivity in Frontal Lobe Epilepsy

Benjamin Klugah-Brown[1] · Cheng Luo[1] · Hui He[1] · Sisi Jiang[1] · Gabriel Kofi Armah[2] · Yu Wu[3] · Jianfu Li[1] · Wenjie Yin[3] · Dezhong Yao[1]

Received: 13 May 2018 / Accepted: 10 September 2018 / Published online: 25 September 2018

Abstract

Frontal lobe epilepsy has recently been associated with disrupted brain functional connectivity; variations among various resting-state networks (RSNs) across time remains largely unclear. This study applied dynamic functional network connectivity (dFNC) analysis to investigate functional patterns in the temporal and spatial domains of various functional systems in FLE. Resting-state fMRI data were acquired from 19 FLE patients and 18 controls. Independent component analysis was used to decompose RSNs, which were grouped into seven functional systems. Sliding windows and clustering approach were used to identify the dFNC patterns. Then, state-specific connectivity pattern and dynamic functional state interactions (dFSIs) were evaluated. Compared with healthy controls, FLE patients exhibited decreased dFNC in almost all four patterns, changes that were mostly related to the frontoparietal system, suggesting a disturbed communication of the frontoparietal system with other systems in FLE. Additionally, regarding the fundamental connectivity pattern (state 3 in this study), FLE showed decreased time spent in this state. Moreover, the duration positively correlated with seizure onset. Furthermore, significantly reduced dynamic connections in this state were observed in the frontoparietal system linked to the cerebellar and subcortical systems. These findings imply abnormal fundamental dynamic interactions and dysconnectivity associated with the subcortical and cerebellar regulation of dysfunctions in frontoparietal regions in FLE. Finally, based on the developed FSI analysis, temporal dynamic abnormalities among states were observed in FLE. Therefore, this altered dynamic FNC extended our understanding of the abnormalities in the frontoparietal system in FLE. The dynamic FNC provided novel insight into the fundamental pathophysiological mechanisms in FLE.

Keywords Frontal lobe epilepsy · Dynamic functional network connectivity · Dynamic functional state interaction · Resting-state fMRI · Double regression

Handling Editor: Louis Lemieux.

Electronic supplementary material The online version of this article (https://doi.org/10.1007/s10548-018-0678-z) contains supplementary material, which is available to authorized users.

✉ Cheng Luo
chengluo@uestc.edu.cn

[1] The Clinical Hospital of Chengdu Brain Science Institute, MOE Key Lab for Neuroinformation, Center for Information in Medicine, School of life Science and technology, University of Electronic Science and Technology of China, No. 4, Section 2, North Jianshe Road, Chengdu 610054, People's Republic of China

[2] Navrongo Campus, Computer Science Department, University for Development studies, P. O. Box 1350, Tamale, Ghana

[3] Department of Radiology, Chengdu First People's Hospital, Chengdu 610031, People's Republic of China

Introduction

Frontal lobe epilepsy (FLE) is characterized by seizures involving the frontal lobes and usually occurs for a certain duration (usually for brief periods) during wakefulness or sleep. FLE occurs in approximately 20–30% of focal epilepsy sufferers (Doelken et al. 2012). Seizures in FLE originate from the frontal lobes and interrupt relative function in frontal regions but may differ in terms of the location involved (Mayo Clinic 2008; Beleza and Pinho 2011) or depending on the functional networks impacted. Seizures in FLE may mostly fall under multi-cognitive defects and motor-related abnormality networks (Kellinghaus and Lüders 2004; Beleza and Pinho 2011). These phenomena implicate abnormality in multiple functional systems in FLE patients. Nonetheless, in contrast to the

other types of epilepsy such as temporal lobe epilepsy, FLE imaging studies are few, which makes it relatively difficult to ascertain the functional network diversities and behavioural correlates across the whole brain, thereby obscuring clarity.

Recently, neuroimaging methods have started to become increasingly employed to understand epileptic disorders across various modalities; for example, EEG-fMRI has been used to localize the potential original regions of seizures in FLE (An et al. 2015). In addition, imaging methods have been used to delineate the focal regions of seizures suggested to have different functional connectivity patterns in FLE patients (Luo et al. 2014). Resting-state functional connectivity has also been used to explore the connectivity alterations within resting-state networks (RSNs) in various types of epilepsy (Luo et al. 2015; Tracy and Doucet 2015; Jiang et al. 2017; Zhong et al. 2018). Functional network connectivity (FNC) has been used to identify the connectivity between networks from different point of views (Jafri et al. 2008) and has also been applied in epilepsy and other diseases to uncover the coupling among RSNs (Luo et al. 2012; Tan et al. 2015; Li et al. 2017a, b). Even so, all of these methods mentioned focus on the static relationship within or between brain networks, and these methods have recently been challenged by fundamental models. Thus, static connectivity basically only measures brain activities averaged over time during resting scans. Consequently, the resulting static connectivity has been suspected to mask various states of dynamic connectivity (Rashid et al. 2014; Graña et al. 2017) occurring within the individual brains. In light of this, the current study focused on the use of windowed dynamic FNC to investigate differences that occur between various networks during resting-state in both the temporal and spatial domains.

Dynamic functional connectivity has been proposed to be eminent throughout rest (Deco et al. 2013). Studies using dynamic methods have shown that not only do subtle events exist at rest but also certain statistical properties are inherent. Extensive analyses, such as those done by Chang and Glover (2010), suggested that significant differences in resting information observed in the posterior cingulate cortex were the result of dynamic events observed using the wavelet-based continuous frequency but not necessarily by static properties. Other studies have used sliding window correlational approaches to observe the dynamic functional connectivity (Damaraju et al. 2014; Rashid et al. 2014) in the brains of both patients and healthy individuals. Consequently, the field of dynamic FNC has widened in regard to characterizing such differences, particularly during the disease resting-state in patients. In epilepsy, the interictal epileptic discharges are often transient for propagation in different regions and affects the multi-systems. Dynamic FNC might therefore provide complimentary, if not fresh, insight into the underlying pathophysiological mechanisms in patients.

To our knowledge, this is the first time windowed dynamic connectivity among RSNs has been applied to FLE data to explore the temporal and spatial patterns. We used a clustering approach and exploratory methods to determine the dynamic FNC of the derived temporal and spatial matrices.

Materials and Methods

Participants

In this study, we used resting-state fMRI experimental data collected from 37 participants, including a total of 19 FLE patients [nine females; mean age = 24.2 years; standard deviation = 9.5 years; age range 13–51 years; number of patients with unilateral interictal epileptic discharges (IED) = 4 (left) and 6 (right), number of patients with bilateral IED = 9] recruited from the Clinical Hospital of Chengdu Brain Science Institute (CBSI), University of Electronic Science and Technology of China (UESTC). All patients were diagnosed by neurologists based on the clinical information in accordance with the International League Against Epilepsy (ILAE) guidelines (Engel and International League Against Epilepsy (ILAE) 2001). Routine CT and MRI examinations did not show any structural aberrations in the FLE patients. Detailed demographic information (such as; age of epilepsy onset, Interictal EEG, seizure type, medication, family history of epilepsy) can be found in Table S1 (Online resource). The dataset used in this study is same as our previous research (Dong et al. 2016). In addition, 18 age and gender-matched, healthy participants were also recruited (five females; mean age = 23.9 years; standard deviation = 8.9 years; age range 11–41 years). All approaches and the study procedure were approved by the local Ethics Committee of UESTC. We also required that written approval forms be submitted by each participant. All subjects provided written consent to participate in this study. Part of the consent included the exact information about the scanning procedure and psychological assessment. The study was approved by the Ethics Committee of the clinical hospital of CBSI in accordance with the Declaration of Helsinki.

Imaging Parameters

All MRI data were collected using an MRI scanner (3.0T, Discovery MR750, GE, USA) in The Clinical Hospital of Chengdu Brain Science Institute of UESTC. T1-weighted anatomical images were collected using a three-dimensional fast spoiled gradient-echo (3D FSPGR) sequence, and the scanning parameters were as follows: slices = 152; TR/

TE = 6.008 ms/1.984 ms; field of view = 256 × 256 mm^2; flip angle = 9°; matrix size = 256 × 256 and slice thickness = 1 mm (no gap). The functional images were collected using a gradient-echo echo-planar imaging sequence. The scanning parameters were as follows: slices = 35; TR/TE = 2000 ms/30 ms; field of view = 240 × 240 mm^2; flip angle = 90°; matrix size = 64 × 64 and thickness = 4 mm. A total of 255 volumes were obtained over a 510-s period. During the resting-state fMRI scanning, all subjects were explicitly instructed to close their eyes and relax without falling asleep.

Preprocessing and Independent Component Analysis of fMRI

For functional images, the first five (5) volumes were discarded to remove the T1 saturation effects, followed by slice timing, realignment, spatial normalization (3 × 3 × 3 mm^3) and smoothing [6-mm full-width at half maximum (FWHM)] representing the preprocessing steps. Our analysis was performed by using a combination of toolboxes, including the fMRI toolbox found in the SPM8 software, (http://www.fil.ion.ucl.ac.uk/spm/software/spm8/), neuroscience information toolbox (Dong et al. 2018) for preprocessing and the group ICA (GICA) toolbox in the GIFT (http://mialab.mrn.org/software/gift/) for independent component analysis of fMRI. Data collected were thresholded at translation < 2 mm and rotation < 2° to avoid extreme head motion, which is known to introduce noise. The removal of the possible nuisance was done as follows: nuisance signals, which included linear trend, head motion, and the individual means of the white matter and cerebrospinal fluid signals, were excluded from the fMRI data through multiple linear regression analysis; Besides, framewise displacement (FD) was evaluated in the two groups (Power et al. 2012). The FD for each participant was evaluated using the following formula;

$$FD = \frac{1}{T-1}\sum_{i=2}^{T}\sqrt{|\Delta d_{x_i^1}|^2 + |\Delta d_{y_i^1}|^2 + |\Delta d_{z_i^1}|^2 + |\Delta d_{x_i^2}|^2 + |\Delta d_{y_i^2}|^2 + |\Delta d_{z_i^2}|^2} \quad (1)$$

where T is the number of the fMRI time points, and $x_i^1/x_i^2, y_i^1/y_i^2$ and z_i^1/z_i^2 are translations/rotations at the ith time point in the x, y and z directions, respectively; $\Delta d_{x_i^1 = x_i^1 - x_{i-1}^1}$.

We adopted GICA to analyse all the data from both the patients and healthy subjects. We then decomposed all data resulting in linear combinations representing distinct timecourses. For us to achieve better components corresponding to anatomical and functional segments, we applied a high model order of 100 components. The Infomax algorithm was used for ICA estimation and was repeated 20 times in ICASSO in other to identify stable and consistent components. We then selected intrinsic components based on peak activation in the grey matter, low spatial overlap and low TC frequency fluctuations.

Functional Network Divisions

During the ICA decomposition, we used a high model order to obtain the functional parcellation, where the number of components, $C = 100$. The model was used to decompose functional regions that exhibited temporal coherency. We retained 150 principal components (PCs) during the principal component analysis for subject-specific data reduction. Furthermore, the expectation maximization algorithm, implemented in the GIFT toolbox, was used to retain $C = 100$ principal components during the group data reduction.

After ICA was performed, the following two steps were taken: (1) 50 ICs were selected from 100 ICs and then grouped into seven network systems based on the spatial distribution of each IC; and (2) the timecourse of each selected IC was processed, and was further used to calculate static FNC (sFNC).

Here, 50 ICs were selected based on peak activation clusters in the grey matter with little or no overlap within the white matter and other areas, such as the edges of the brain and ventricles; this was done through the inspection of spatial maps, as well as of the associated timecourses. We bandpass filtered the processed timecourses for the RSNs with a high frequency cut-off of 0.15 Hz; this was done to ensure the removal of the effects of scanner drift, as well as movement variations, we then inspected the power spectra (ratio of low to high frequencies) of each IC, components with frequencies higher than 0.15 Hz and lower than 0.01 Hz were excluded and reordered to fit the arrangement of the FNC matrix based on their anatomical and known functional properties, specifically for perceptual and higher cognitive networks, which resulted in an ordered row division including the default mode network (DMN), subcortical network (SCN), auditory network (ADN), frontoparietal network (FPN), visual network (VSN), cerebellar network (CRN), and sensorimotor network (SMN). The intrinsic components were grouped into seven brain networks for further analysis (Allen et al. 2011). We used the seven networks order to estimate the sFNC matrix in a way similar to our previous studies (Luo et al. 2012; Li et al. 2015; Jiang et al. 2018).

FNC with Sliding Window and Clustering Analysis

We employed a sliding window approach (Allen et al. 2011) to evaluate the dynamic FNC patterns for all subjects. We computed correlations between the selected ICs with a window width size of 22 TRs = 44 s and sliding steps = 1, resulting in 228 windows. The 228 windows were obtained for all 37 subjects; thus, there were $228 \times 37 = 8436$ instances. To ensure a complete covariance matrix and sparsity, we set constraints on the L1 norm by using the graphical LASSO. Each subject's regularization parameter was evaluated by independently optimizing lambda to ensure capture of unseen data.

We used all the windows of the temporal matrices between the RSNs and applied the k-mean clustering algorithm to obtain a set of discrete cluster centroids. The k-mean clustering was used because the model of dynamic connectivity repeats within subjects across time. We selected k from 2 to 10 representing cluster states. In each selection state, the clustering algorithm was repeated 500 times to increase the odds of escaping local minima for clustering by using different distance functions, which produced similar results with $(50 \times (50-1))/2 = 1225$. To obtain the optimal number of cluster centroids, we used the Gap statistic, elbow criterion and Silhouette algorithms. Consequently, $k = 4$ was obtained from the elbow criterion (this result was selected because the results from the other two methods gave less than three states, i.e. $k = 2$, also four clusters represented more differences, which is better for pattern evaluation compared to only two clusters. Thus, more clusters will give more interacting FC among states and can be used to find abnormal functions in patients) and the medians are presented as FCs for each state capturing all features. A subject median was estimated for each cluster division obtained from the subject windows, representing the connectivity of subjects for each state.

In addition, we used the transition state vectors computed from the dynamic FNC matrices of the windows of the IC timecourses to compute the dwell time (average number of successive windows in the same state) and fraction of time (proportion of all windows) in each state. The evaluations of group difference using these state vectors were done through rank-sum, non-parametric tests (data were not distributed around the means of the windows, and we were interested in finding which group was more or less than the other), and the threshold was set as $p < 0.05$. Furthermore, we proceeded to estimate the differences in variation of the dwell time across subject for each state, here, we computed the variances by taking the standard deviations of all subjects within each group. The variance of each state was then compared through non-parametric permutation test with random repetition of 1000 times, the test was run for four times which resulted in four p values threshold at $p < 0.05$. Moreover, to estimate the difference in variation of dwell time across states for each subject, we computed the standard deviation across the four clusters within each subject, this resulted in two vectors (each column and row representing a group and the variability for each subject respectively), then the difference between patients and HC was calculated through two sample t-test ($p < 0.05$).

Individual Dynamic FNC Analysis Using Double Regression

Here, we adopted the double regression approach as an exploratory method to back-construct individual states (spatial weights) and their dynamic variation across sliding windows (temporal features). This method, as described in (Beckmann et al. 2009), is widely used in back-construction processing in group ICA analysis to define the timecourses and intrinsic independent components within each subject.

We applied the double regression method as follows:

First regression step:

$$Y = \beta_1 X_1 + \varepsilon \tag{2}$$

where Y epresents the individual FNC matrix of each sliding window, and X_1 indicates the matrices for the four states obtained from the clustering mentioned above, which reflects the spatial pattern of states. Thus, β_1 represents the temporal feature, that is, the dynamic variation in the weight of a given state across sliding windows in the individual level. ε signifies the error term.

Second regression step:

Here, β_1 was included as a regressor to identify the individual spatial weight of each state in all sliding windows.

$$Y = \beta_2 X_2 + \varepsilon \tag{3}$$

where Y was set as the individual FNC matrix of each sliding window, and X_2 equals β_1 in the first regression step. Thus, β_2 represents the distinct spatial weight of each state, which reflects the individual dynamic FNC of each state.

Finally, we computed the correlation of β_1 to reflect dynamic functional interactions between states (dFSI) at the individual level. We used a non-parametric statistical analysis through permutation tests to evaluate the differences in dFSI between the two groups. Here, the dFSI matrix demonstrates a high-order correlation and reveals the pattern of the inter-state connectivity. The dynamic FNC (spatial weight of each state, β_2) values were also compared between groups using non-parametric (the observed data were not normally distributed about the means) statistical analysis.

Correlation Analysis

The between-group significance obtained, marked by the temporal state matrices, was followed up by a correlation

analysis between the state vectors and the clinical features of epilepsy (age of onset), while controlling for gender. The correlation analysis was done through partial correlation with $p < 0.05$ (FDR-corrected). We utilized the partial correlation function in the MATLAB13b software.

In summary, Fig. 1 illustrates the analytical procedure involved in the process used in generating our results, involving data processing, ICA decomposition for the selection of intrinsic RSNs, and dynamic FNC matrices were computed within all windows for each subject, followed by clustering analysis to generate state matrices for temporal and spatial analyses. State matrices were evaluated in the temporal domain, and the double regression method was employed to estimate the spatial matrices.

Results

Seven Functional Networks

Out of the 100 components decomposed, we identified seven networks composed of 50 IC groups based on their anatomical and functional features, as shown in Fig. 2a, namely, nine default mode network components (DMN-ICs 14, 15, 18, 32, 33, 34, 37, 43 and 48), four subcortical network components (SCN-ICs 4, 6, 17 and 24), four auditory network components (ADN-ICs 29, 41, 61 and 65), 14 frontoparietal network components (FPN-ICs 5, 7, 9, 11, 12, 13, 22, 23, 25, 28, 30, 31, 99 and 100), nine visual network components (VSN-ICs 19, 21, 36, 39, 40, 52, 90, 97 and 98), five cerebellar network components (CRN-ICs 10, 16, 42, 50 and 60) and five sensorimotor network components (SMN-ICs 26, 27, 35, 38 and 51). The RSNs in the various networks are arranged in the circular order shown in Fig. 2b. The T-maps and power spectra information of the selected components are shown in Fig. 1 (Online Resource). Table S2 (Online Resource) shows the peak activation for the all the ICs across the seven networks. The between-group differences in the sFNC are shown in Fig. 2 (Online Resource).

Clustering and Dynamic FNC Patterns

Four FNC patterns were identified for the FNC matrices from the sliding window analysis, and the temporal matrices from the clustering resulted in FC within the subject data, which were arranged in order of occurrence from $k = 2 - 10$, as shown in Fig. S3a (Online Resource). The elbow criterion resulted in $k = 4$, as shown in Fig. S3b (Online Resource). The group-specific median of the clustering for all subjects in each of the four states is shown in Fig. S4a (Online Resource), indicating the cluster centroid, which specifies the FC, and the percentages attached to the centroids (medians) represent the ratio of the number of occurrence per state to the total number of sliding windows. Fig. S4b and c (Online Resource) are the group-specific centroids for the FLE patients and healthy subjects, respectively. In addition, the 1% connections with high-cluster amplitudes in each state are shown in Fig. S5 (Online Resource). From Figs. S4 and S5 (Online Resource), we found that state 1 showed major connections among the SMN with the DMN and others; the main links in state 2 related to the high-level networks (DMN and FPN); state 3 showed general communication among all of seven networks with the highest percentage (33%), which represents the fundamental connection pattern in the whole brain that facilitates specific patterns of brain activation; and the main connections in state 4 were located in the FPN, CRN and VSN.

Furthermore, between-state differences obtained in the dwell time analysis showed that, compared with healthy controls, FLE patients exhibited significantly brief average dwell times ($p = 0.0026$), and a fraction of the duration ($p = 0.0021$) in state 3 is shown in Fig. 3a, b.

In addition, we found significant difference in the computed variations of the dwell time across subjects for each state (compared with HC, patients were lower, $p = 0.044$, in state 3). Besides, there was no significant difference in the subject variability across states ($t_{df=35} = 0.346$, $p < 0.731$), where df = degree of freedom.

We observed a significant positive correlation ($p = 0.003$) between the percentage mean dwell time in state 3 and the clinical feature (Age of onset) shown in Fig. 3c, whereas we found no correlation between the other state vectors and the clinical scores.

Individual Dynamic FNC

Through the non-parametric tests, we found major altered spatial patterns of dynamic FNC in patients for the four states: (1) For state 1, we found increased connections in FPN-SCN (IC9-IC6) and FPN-CRN (IC22-IC42) as well as decreased connections in FPN-SCN (IC5-IC6), FPN-SMN (IC9-IC35), ADN-FPN (IC61-IC100) and FPN-CRN (ICIC100-IC60). All of them connected to the FPN. (2) In state 2, increased connections were found in DMN-SMN (IC48-IC51), and decreased connections were also found in SCN-FPN (IC24-IC100), ADN-VSN (IC65-IC39), FPN-SMN (IC9-IC27), FPN-CRN (IC12-IC16), and DMN-SMN (IC37-IC26). (3) In state 3, an increased relationship was found in DMN-SMN (IC48-IC27), with more decreased connections in FPN-SCN (IC7-IC4), FPN-CRN (IC7-IC16), FPN-SCN (IC12-IC6), FPN-SCN (IC22-IC6), FPN-CRN (IC22-IC10), FPN-CRN (IC28-IC42) and FPN-CRN (IC31-IC42). (4) Finally, in state 4, we found only decreased connections in SCN-SMN (IC4-IC51), SCN-SMN (IC24-IC51), FPN-SCN (IC11-IC24), FPN-VSN (IC11-IC52), FPN-CRN (IC12-IC16), VSN–VSN (IC52-IC98) and VSN-SMN

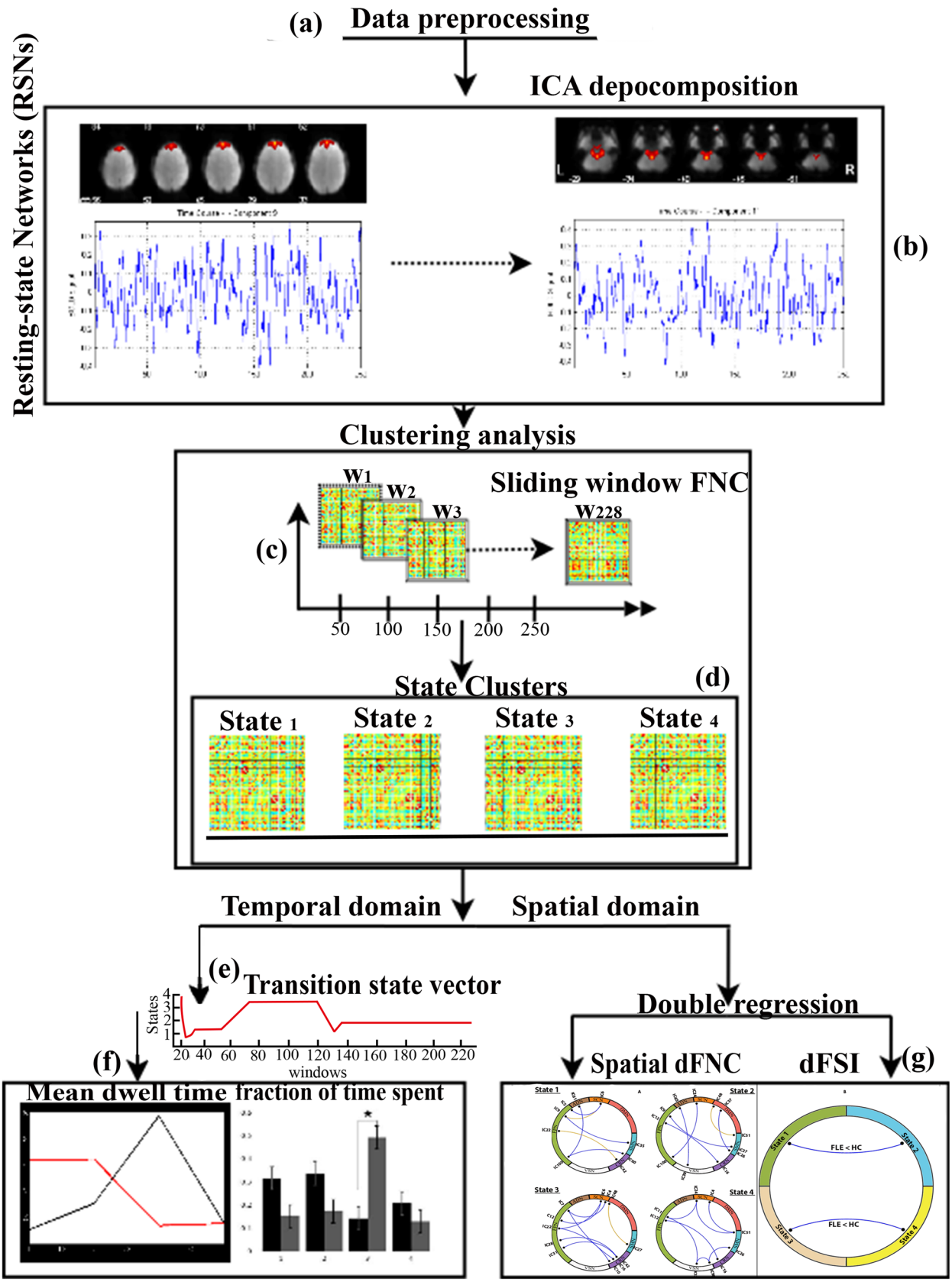
(a) Data preprocessing
ICA depocomposition
Resting-state Networks (RSNs)
(b)
Clustering analysis
Sliding window FNC
W1
W2
W3
W228
(c)
50 100 150 200 250
State Clusters
(d)
State 1
State 2
State 3
State 4
Temporal domain
Spatial domain
(e) Transition state vector
States
windows
Double regression
(f)
Mean dwell time
fraction of time spent
Spatial dFNC
dFSI
(g)
FLE < HC
FLE < HC

◂**Fig. 1** An overview of the analysis steps of dynamic functional network connectivity. The analysis included the following steps: **a** preliminary resting-state fMRI data were preprocessed; **b** ICA decomposition was performed, and 50 intrinsic RSNs were selected **c** dynamic FNC matrices were computed within all windows for each subject; **d** clustering and state analyses were performed to evaluate the dynamic FNC changes; **e** transition state vectors were obtained through the calculated membership assignments for all windows; **f** temporal state vectors were then computed and could be viewed for all states; and **g** exploratory analysis was conducted from the state matrices, yielding patterns within each state between the two groups. Abbreviations, dFSI, dynamic functional state interactions; dFNC, dynamic functional network connectivity

(IC98-IC26). These patterns are shown in Fig. 4a. In short, we found 70% altered connections (19/27) related to the FPN; particularly, all of the decreased connections in state 3 (seven links in eight altered connections) were located in the FPN linked to the CRN and SCN. Moreover, the following observations were made in dFSI among the four states: we observed a significantly reduced relationship between states 1 and state 2, as well as a reduced relationship between states 3 and state 4, as shown in Fig. 4b.

Discussion

We explored dynamic FNC using a sliding-window approach to estimate the changes between FLE patients and healthy subjects. Four dynamic FNC patterns were identified across all subjects. Moreover, evaluations were performed within the temporal and spatial domains of the subject matrices for four patterns. Consequently, the following findings were revealed: (1) Compared with healthy subjects, FLE patients demonstrated major reductions in dynamic FNC in almost all of the patterns. Interestingly, 70% of the decrease was related to the FPN, suggesting disturbed communication of the frontoparietal system with other systems in FLE. (2) For the fundamental connection pattern (state 3), FLE showed decreased dwell time in windows and fractions of time spent in this state. Additionally, the duration spent by patients in this state positively correlated with seizure onset. In addition, significantly reduced dynamic connections in this state were observed in the FPN linked to CRN and SCN. These findings implied abnormal dynamic interactions in the fundamental connective pattern in FLE, and also the dysconnectivity between the frontoparietal system with cerebellum and subcortical nuclei contributed to the major abnormalities in this state. (3) Finally, the novel exploratory analysis showed significantly reduced relationships among the states across all sliding windows in FLE. To the best of our knowledge, this study was the first to demonstrate significant differences in the dynamic FNC between FLE patients and controls. The approach, therefore, provided novel insight into the fundamental pathophysiological mechanisms of the frontoparietal system in FLE.

FNC, as a method of exploring functional alterations and interactions among resting-state networks, has been the focus of neuroimaging research recently. It is an important method to statistically analyse whole-brain networks, particularly mechanisms and changes in neuropsychiatric disorders (Jafri et al. 2008; Wang et al. 2015). The sFNC approach depends on the notion that functional connectivity is due to the static nature of features over time during scanning. Some studies (Li et al. 2015, 2017a, b) used sFNC to investigate alterations in epilepsy. In FLE, the propagation of epileptic activation might influence multiple regions that differ from the common RSNs in healthy controls (Luo et al. 2014). In the current study, the static connectivity showed significant group differences between the SMN and the VSN, networks that are primary involved in sensory perception, as well as motor processes. This finding might indicate primary perceptual discrepancies in FLE. Furthermore, our study explored dynamic matrices and found that FLE patients demonstrated major reductions in dynamic FNC in almost all patterns. In epilepsy, the dynamic analysis would contribute to uncovering the propagation path of epileptic activity and seizures prediction (Direito et al. 2017) and detection (Li et al. 2016; Geier and Lehnertz 2017).

Thus, these findings extended the previous static dysconnectivity to disturbed dynamic connectivity in FLE and provided more evidence for understanding the dysfunctional connectivity mechanisms in FLE. Interestingly, 70% of the decreased connections were related to the FPN, and the disturbed communication between the frontoparietal system and other systems played a key role in the general abnormalities in the whole brain of FLE to some extent. In addition, cognitive defects are often found in FLE (Williamson and Jobst 2000; Fletcher and Henson 2001; Exner et al. 2002; Braakman et al. 2013; Dong et al. 2016). Several investigations have suggested that profound cognitive activities underlie resting experimental changes in the functional connectivity pattern (McAvoy et al. 2008). Hence, evidence directed towards the dynamic processes and sudden brain changes that occur in functional connectivity in a time-varying manner increasingly make this approach worth applying (Shen et al. 2015). Consistent with this presumption, abnormalities in the frontoparietal system within the temporal and spatial domains, demonstrated in FLE here, would implicate the relationship with behavioural cognitive alterations in FLE.

According to the connective pattern and state percentage resulting from the cluster of dynamic FNC, state 3 with widespread connections in all seven networks, might reflect a fundamental connection pattern in the whole brain, which would facilitate a specific pattern of brain activation. Our study explored dynamic matrices obtained from temporal

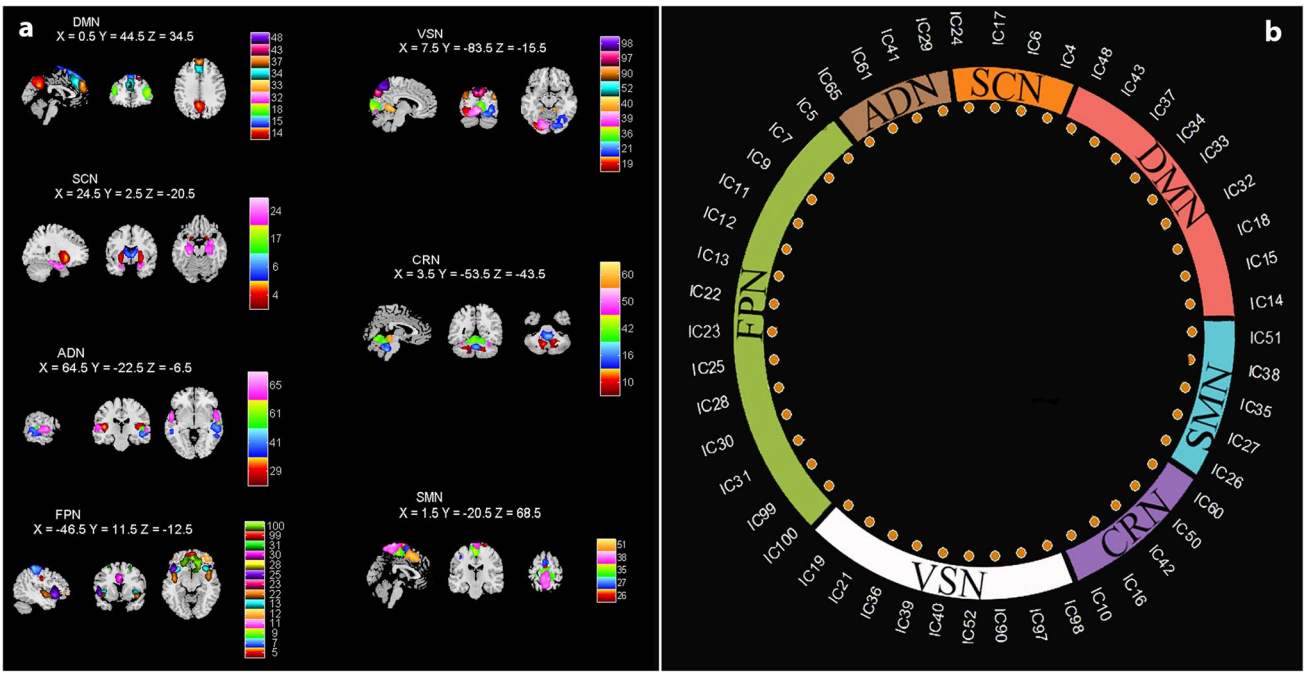

Fig. 2 Identified network systems. **a** RSNs arranged into seven subcategories. Each color in the composite map matches a different ICN. **b** Network arrangement used in the subsequent analysis of the RSNs

state vectors within the temporal domain to uncover state-specific alterations. FLE patients had shorter durations than the controls across the windows and spent less time in state 3, with no significant differences in the other states. Besides, the variability of dwell time across subjects also indicated patients had lower variability than healthy controls in state 3. In addition, positive correlations between the mean dwell time of this state and seizure onset were observed, suggesting that early seizure onset leads to more severe effects on this state. Similar to the reduced relationship mentioned above, patients demonstrated reduced FC patterns in this state, including two profound aspects, namely, connections indicating that modulations exist between the frontal lobe and subcortical nuclei processes, as well as fronto-cerebellar networks (Braakman et al. 2013) found in FLE. Here, the SCN consisted of the putamen and caudate, which play important roles in the regulation of epileptic discharges (Norden and Blumenfeld 2002). Abnormalities, including epileptic activities, located within the frontoparietal areas may be responsible for mental dysfunctions in FLE patients (Exner et al. 2002; Braakman et al. 2011). In this study, the decreased connection between the frontal-subcortical network fundamental connection patterns suggested the modulation of subcortical nuclei of the frontoparietal system, which might be responsible for the altered dynamic function, consistent with previous studies. In addition, studies have found the cerebellar role and its interactions with epileptic discharges (Kros et al. 2015a, b). In our study, the decreased contribution of the spatial dynamic FC of the fundamental state might have influenced the dynamic modulation by the FPN and cerebellum of the epileptic activity in FLE patients. Collectively, these results revealed the abnormal dynamic functional architecture in the fundamental connection patterns, reflecting the base pathophysiological mechanisms of FLE. In addition, the subcortical nuclei and cerebellum played crucial roles in the interaction with the frontoparietal system, implicating basal ganglia and cerebellar regulation of epileptic discharges in FLE.

Apart from the analysis within the spatial domain, we identified relationships corresponding to the dynamic spatial pattern among states across windows. A state-related timecourse was constructed to describe the contribution of each state to the dynamic matrices in the temporal domain using a double regression analysis. The timecourse related to each FC state can be different from the timecourses associated with the independent components derived directly from BOLD rs-fMRI data using ICA. The BOLD re-fMRI related timecourses were used to calculate sFNC and would reflect the contribution of a given state for the time-varying FNC matrices. Besides, the dynamic functional state interaction (FSI) reflects the temporal coupling of all states, which represented high-order dynamic features of functional networks. The high-order correlation is similar to those proposed in previous studies (Xiaobo et al. 2016; Zhang et al. 2017). Essentially, this was the first study to evaluate the FSI of each state timecourse in patients with epilepsy. Here, we

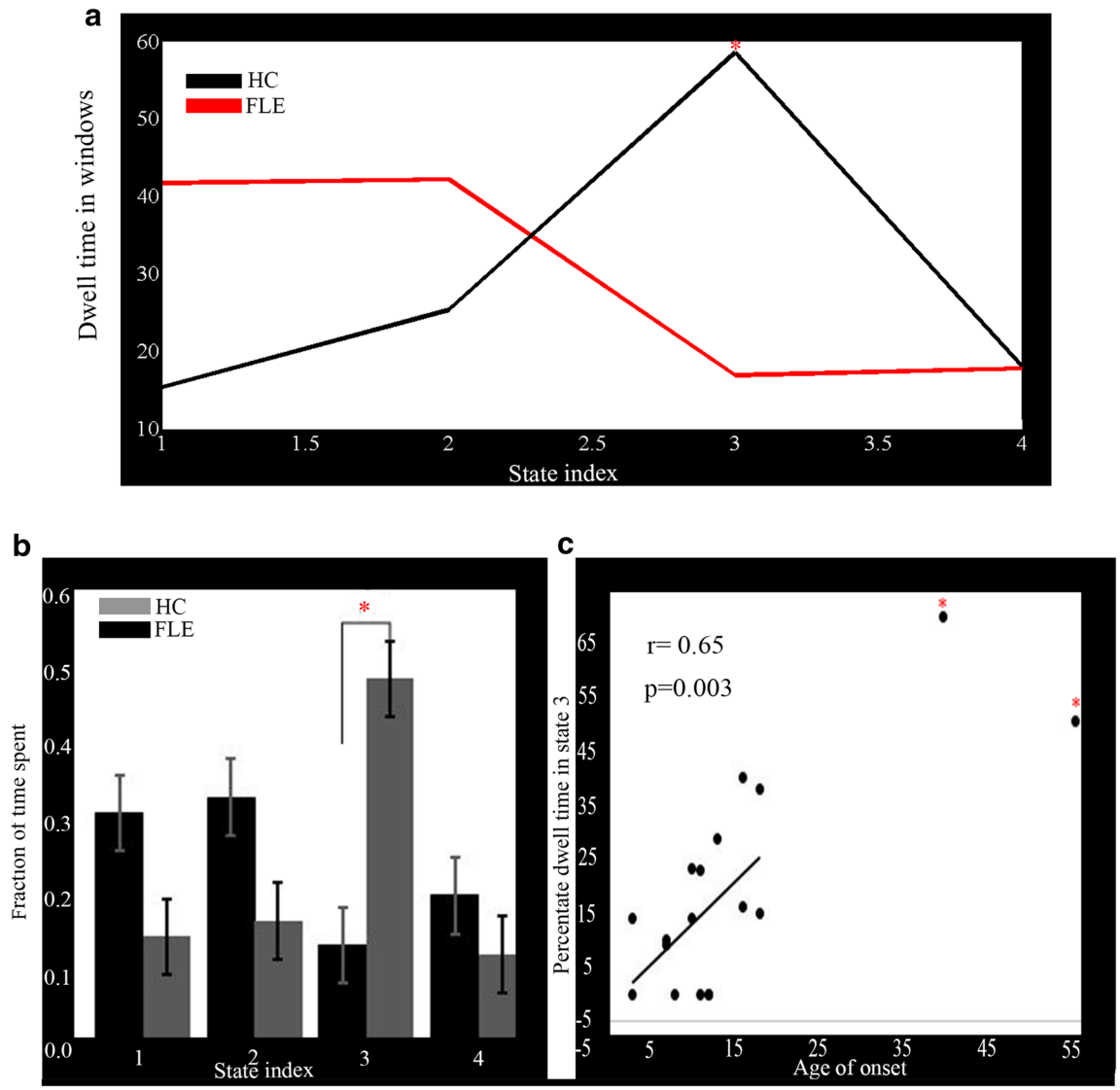

Fig. 3 Group differences in the temporal metrics obtained from state transition vectors. The asterisk(*) in the bar plots signifies statistically significant differences between the two groups. Error bars represent the standard error of the group differences between groups obtained from the state transition vector **a**: mean dwell time, **b**: fraction of time spent in each state, and **c**: correlation between percentage dwell time and age of onset. *Indicates outliers, which were not included in the correlation analysis

observed reduced FSI between states 1 and 2 as well as between states 3 and 4, in FLE. Besides, this study provided more evidence to understand the disrupted dynamic functional connectivity in FLE patients.

Although this study brought to light the ability of dynamic FC as a means of evaluating FNC in a whole-brain analysis, during this study, a number of constraints were evident. (1) The sample size of the patients for our RSN analysis was relatively small. This limitation resulted in our inability to apply certain methods, such machine learning, to further characterize the dynamic features. Therefore, we suggest a reasonably larger dataset in future studies. (2) Though the ICA analysis, subsequent sliding windows and noise removal was supposed to separate the artefacts, such as head motion and heart beat rates, from the components; we were not able to do a thorough artefact removal analysis, which may have influenced our FC results. Finally, k-mean clustering, as used in this study, comes with various limitations, such as issues that have to do with size, density and when a dataset has outliers. As a result, we hope that our next study will include other clustering methods proven to be much more efficient than k-mean clustering.

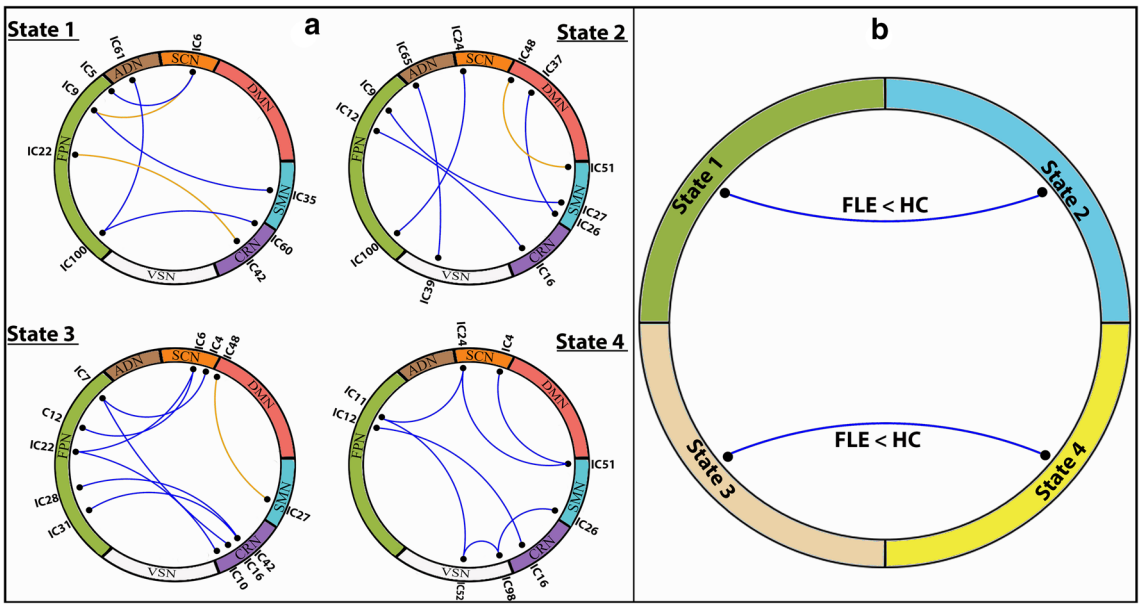

Fig. 4 Double regression analysis for all subjects across the windows in each state. **a** shows the contributing FC. Connecting lines indicate the FC between the ICs contributing to each state. Blue and yellow lines indicate reduced and increased connections, respectively. **b** shows the state timecourse of the dFSI. Blue lines indicate reduced state window FC contributions between states 1 and 2 and 3 and 4, respectively. All connections were threshold at $p < 0.005$

Conclusion

Using dynamic FNC, this study analysed temporal and spatial dynamic connectivity in FLE. FLE patients demonstrated decreased dynamic FNC in almost all states, mainly in the dysfunctional connections between the frontoparietal system and other systems. Additionally, states with fundamental connective patterns were observed in the temporal and spatial dynamic abnormalities in FLE. Interestingly, the cerebellum and basal ganglia had disrupted dynamic interactions with the frontoparietal system in this state, which suggests basal ganglia and cerebellar regulation of epileptic discharges in the frontoparietal lobe in FLE. Finally, based on the developed FSI analysis, which highlighted the capability of temporal dynamic analysis to delineate differences in neurological diseases, the temporal dynamic abnormalities in states were also observed in FLE. This abnormal dynamic FNC therefore extended our understanding of the pathophysiological brain network mechanisms in FLE.

Acknowledgements This work was supported by grants from the National Nature Science Foundation of China (Grant Nos. 81771822, 81471638 and 81330032); The Project of Science and Technology Department of Sichuan Province (Nos. 2017SZ0004 and 2017HH0001); and the '111' project of China (Grant No. B12027). We thank Dr. Jiang and Dr. Wang for their help in collecting data.

Compliance with Ethical Standards

Conflict of interest None of the authors had any conflicts of interest to disclose. We confirm that we have read the Journal's position on the issues involved in ethical publication and affirm that this report is consistent with those guidelines.

References

Allen EA, Damaraju E, Plis SM, Erhardt EB, Eichele T, Calhoun VD (2011) Tracking whole-brain connectivity dynamics in the resting state. Cereb Cortex 24:663–676

An D, Dubeau F, Gotman J (2015) BOLD responses related to focal spikes and widespread bilateral synchronous discharges generated in the frontal lobe. Epilepsia 56(3):366–374

Beckmann CF, Mackay CE, Filippini N, Smith SM (2009) Group comparison of resting-state FMRI data using multi-subject ICA and dual regression. NeuroImage 47:S39–S41. https://doi.org/10.1016/S1053-8119(09)71511-3

Beleza P, Pinho J (2011) Frontal lobe epilepsy. J Clin Neurosci 18(5):593–600

Braakman H, Vaessen M, Hofman P, Debeij-van Hall M, Backes W, Vles J, Aldenkamp A (2011) Cognitive and behavioral complications of frontal lobe epilepsy in children: a review of the literature. Epilepsia 52:849–856

Braakman H, Vaessen M, Jansen J, Debeij-van Hall M, de Louw A, Hofman P et al (2013) Frontal lobe connectivity and cognitive impairment in pediatric frontal lobe epilepsy. Epilepsia 54:446–454

Chang C, Glover G (2010) Time frequency dynamics of resting state brain connectivity measured with fMRI. Neuroimage 50:81–98. https://doi.org/10.1016/j.neuroimage.2009.12.001

Damaraju E, Allen E, Belger A, Ford J, McEwen S, Mathalon D et al (2014) Dynamic functional connectivity analysis reveals transient states of dysconnectivity in schizophrenia. NeuroImage:Clinical 5:298–308

Deco G, Ponce-Alvarez A, Mantini D, Romani G, Hagmann P, Corbetta M (2013) Resting-state functional connectivity emerges from structural and dynamically shaped slow linear fluctuation. J Neurosci 33:11239–11252

Direito B, Teixeira CA, Sales F, Castelo-Branco M, Dourado A (2017) A realistic seizure prediction study based on multiclass SVM. Int J Neural Syst 27(3):1750006. https://doi.org/10.1142/S0129065717500006X

Doelken M, Mennecke A, Huppertz H (2012) Multimodality approach in cryptogenic epilepsy with focus on morphometric 3T MRI. J Neuroradiol 39(2):87–96

Dong L, Wang P, Peng R, Jiang S, Klugah-Brown B, Luo C, Yao D (2016) Altered basal ganglia-cortical functional connections in frontal lobe epilepsy: a resting-state fMRI study. Epilepsy Res 128:12–20

Dong L, Luo C, Liu X, Jiang S, Feng H, Li J, Gong D, Yao D (2018) Neuroscience information toolbox: an open source toolbox for EEG-fMRI multimodal fusion analysis. Front Neuroinform 12:56

Engel J Jr, International League Against Epilepsy (ILAE) (2001) A proposed diagnostic scheme for people with epileptic seizures and with epilepsy: report of the ILAE Task Force on Classification and Terminology. Epilepsia 42(6):796–803

Exner C, Boucsein K, Lange C, Winter H, Weniger G, Steinhoff B, Irle E (2002) Neuropsychological performance in frontal lobe epilepsy. Seizure 11:20–32

Fletcher P, Henson R (2001) Henson, frontal lobes and human memory. Brain 124:849–881

Geier C, Lehnertz K (2017) Which brain regions are important for seizure dynamics in epileptic networks? Influence of link identification and EEG recording montage on node centralities. Int J Neural Syst 27(1):1550035. https://doi.org/10.1142/S0129065715500355

Graña M, Ozaeta L, Chyzhyk D (2017) Resting state effective connectivity allows auditory hallucination discrimination. Int J Neural Syst 27(05):1750019. https://doi.org/10.1142/S0129065717500198

Jafri M, GD P, Stevens M, Calhoun V (2008) A method for functional network connectivity among spatially independent resting-state components in schizophrenia. Neuroimage 39:1666–1681

Jiang S, Luo C, Gong J, Peng R, Ma S, Tan S et al (2017) Aberrant thalamocortical connectivity in juvenile myoclonic epilepsy. Int J Neural Syst. https://doi.org/10.1142/S0129065717500344

Jiang Y, Luo C, Li X, Li Y, Yang H, Li J, Chang X, Li H, Yang H, Wang J, Duan M, Yao D (2018) White-matter functional networks changes in patients with schizophrenia. Neuroimage. https://doi.org/10.1016/j.neuroimage.2018.1004.1018

Kellinghaus C, Lüders HO (2004) Frontal lobe epilepsy. Epileptic Disord 6(4):223–239

Kros L, Eelkman RO, De Zeeuw C, Hoebeek F (2015a) Controlling cerebellar output to treat refractory epilepsy. Trends Neurosci 38(12):787–799. https://doi.org/10.1016/j.tins.2015.10.002

Kros L, Eelkman ROH, Spanke JK, Alva P, van Dongen MN, Karapatis A et al (2015b) Cerebellar output controls generalized spike-and-wave discharge occurrence. Ann Neurol. https://doi.org/10.1002/ana.24399

Li Q, Cao W, Liao X, Chen Z, Yang T, Gong Q et al (2015) Altered resting state functional network connectivity in children absence epilepsy. J Neurol Sci 354(1–2):79–85

Li J, Zhou W, Yuan S, Zhang Y, Li C, Wu Q (2016) An Improved sparse representation over learned dictionary method for seizure detection. Int J Neural Syst 26(1):1750006. https://doi.org/10.1142/S012906571750006X

Li Q, Chen Y, Wei Y, Chen S, Ma L, He Z, Chen Z (2017a) Functional network connectivity patterns between idiopathic generalized epilepsy with myoclonic and absence seizures. Front Comput Neurosci. https://doi.org/10.3389/fncom.2017.00038. (**ecollection**)

Li R, Ji GJ, Yu Y, Yu Y, Ding MP, Tang YL, Chen H, Liao W (2017b) Epileptic discharge related functional connectivity within and between networks in benign epilepsy with centrotemporal spikes. Int J Neural Syst 27(7):1750018. https://doi.org/10.1142/S0129065717500186

Luo C, Qiu C, Guo Z, Fang J, Li Q, Lei X et al (2012) Disrupted functional brain connectivity in partial epilepsy: a resting-state fMRI study. PLoS ONE 7:e28196

Luo C, An D, Yao D, Gotman J (2014) Patient-specific connectivity pattern of epileptic network in frontal lobe epilepsy. Neuroimage Clin 4:668–675

Luo C, Zhang Y, Cao W, Huang Y, Yang F, Wang J et al (2015) Altered structural and functional feature of striato-cortical circuit in benign epilepsy with centrotemporal spikes. Int J Neural Syst 25(6): 1550027

Mayo Clinic (2008) Mayoclinic. http://Mayoclinic.com. Accessed Sept 2017

McAvoy M, Larson-Prior L, Nolan T, Vaishnavi S, Raichle M, d'Avossa G (2008) Resting states affect spontaneous BOLD oscillation in sensory and paralimbic cortex. J Neurophysiol 100:922–931

Norden A, Blumenfeld H (2002) The role of subcortical structures in human epilepsy. Epilepsy Behav 3:219–231

Power JD, Barnes KA, Snyder AZ, Schlaggar BL, Petersen SE (2012) Spurious but systematic correlations in functional connectivity MRI networks arise from subject motion. Neuroimage 59:2142–2154

Rashid B, Damaraju E, Pearlson GD, Calhoun VD (2014) Dynamic connectivity states estimated from resting fMRI Identify differences among Schizophrenia, bipolar disorder, and healthy control subjects. Front Hum Neurosci 8:897. https://doi.org/10.3389/fnhum.2014.00897. (**eCollection 2014**)

Shen K, Hutchison R, Bezgin G, Everling S, McIntosh A (2015) Network structure shapes spontaneous functional connectivity dynamics. J Neurosci 35:5579–5588

Tan Y, Tan J, Deng J, Cui W, He H, Yang F et al (2015) Alteration of basal ganglia and right frontoparietal network in early drug-naive Parkinson's disease during heat pain stimuli and resting state. Front Hum Neurosci 9:467

Tracy J, Doucet G (2015) Resting-state functional connectivity in epilepsy: growing relevance for clinical decision making. Curr Opin Neurol 28(2):158–165

Wang L, Liu Q, Shen H, Li H, Hu D (2015) Large-scale functional brain network changes in taxi drivers: evidence from resting state fMRI. Hum Brain Mapp 36:862–871

Williamson P, Jobst B (2000) Frontal lobe epilepsy. In: Williamson P, Siegel A, Roberts D, Thadani V, Gazzaniga M, (eds) Advances in neurology. Raven Press, Philadelphia pp 215–251

Xiaobo C, Han Z, Yue G, Chong-Yaw W, Gang L, Dinggang S, the Alzheimer's Disease Neuroimaging Initiative (2016) High-order resting-state functional connectivity network for MCI classification. Hum Brain Mapp 37: 3282–3296

Zhang H, Chen X, Zhang Y, Shen D (2017) Test-Retest Reliability of "high-order" functional connectivity in young healthy adults. Front Neurosci 11:439. https://doi.org/10.3389/fnins.2017.00439

Zhong C, Liu R, Luo C, Jiang S, Dong L, Peng R, Guo F, Wang P (2018) Altered structural and functional connectivity of juvenile myoclonic epilepsy: an fMRI study. Neural Plast. https://doi.org/10.1155/2018/7392187